Chemical Engineering Journal 200–202 (2012) 480–490

Contents lists available at SciVerse ScienceDirect

Chemical Engineering Journal

journal homepage: www.elsevier.com/locate/cej

Adsorption performance and mechanism of Cr(VI) using magnetic PS-EDTA resin from micro-polluted waters

Ning Mao, Liuqing Yang, Guanghui Zhao, Xiaoli Li, Yanfeng Li *

State Key Laboratory of Applied Organic Chemistry, College of Chemistry and Chemical Engineering, Institute of Biochemical Engineering & Environmental Technology, Lanzhou University, Lanzhou 730000, PR China

HIGHLIGHTS

- A novel magnetic chelating resin with EDTA functionality was prepared.
- It shows easy separation and excellent adsorption for Cr(VI) in aqueous solution.
- 100% of Cr(VI) could be removed at the low metal concentration (<40 mg/L).
- XPS shows that the mechanism contains Cr(VI) reduction and electrostatic interaction.
- A conceptual model for Cr(VI) adsorption by this resin is proposed to illustrate the mechanism.

ARTICLE INFO

Article history:
Received 6 April 2012
Received in revised form 20 June 2012
Accepted 20 June 2012
Available online 28 June 2012

Keywords:
Magnetic resin
Hexavalent chromium
Adsorption

ABSTRACT

Adsorption of Cr(VI) from aqueous solution onto a magnetic chelating resin with EDTA functionality (magnetic PS-EDTA) was investigated in a batch system. Various factors affecting the uptake behavior such as pH, contact time, initial concentration of the metal ions and dosage of resins on Cr(VI) removal were studied. The magnetic modified resin showed higher adsorption capacity and shorter adsorption equilibrium time for Cr(VI) compared with the raw PS-EDTA resin. The equilibrium data were analyzed using the Langmuir, Freundlich and Tempkin isotherm models among which Langmuir isotherm model was found to be suitable for the monolayer adsorption process. The monolayer adsorption capacity values of 123.05 mg/g for raw PS-EDTA and 250.00 mg/g for magnetic resin were very close to the maximum capacity values obtained at pH 4.0. Kinetic studies showed that the adsorption followed a pseudo second-order reaction. The mechanism was further identified by fitting intraparticle diffusion and McKay plots. The result indicates film diffusion was the rate-limiting step and intraparticle diffusion was also involved in adsorption. XPS spectra confirmed that reduction of Cr(VI) by Fe_3O_4 nanoparticle on the resin occurred, while the electrostatic interaction between protonated amine groups and Cr(VI) anion played an important role in the adsorption. Furthermore, the resin could be regenerated through the desorption of the Cr(VI) anions using 0.5 M NaOH solution and could be reused to adsorb again.

1. Introduction

Many industries such as electrodeposition, leather manufacturing, steel production and wood preservative industries generate a huge amount of toxic metals. The discharge of such effluents cause increased adverse effects on human beings and environment. Chromium is one of the most important toxic metals which could damage upper respiratory tract and has chronic toxicity [1]. Chromium exists in trivalent (Cr(III)) and hexavalent (Cr(VI)) states. Cr(VI) has been considered more hazardous to public health due to its mutagenic and carcinogenic properties [2]. It is a relatively strong chemical oxidant and could react with the enzymes of the body or biological systems, resulting that its toxicity is about 300 times more than Cr(III) [3].

Because of its high toxicity, Cr(VI) must be substantially removed from the wastewater before being discharged into the aquatic system. Various methods of chromium removal include chemical reduction, filtration, precipitation, adsorption, electrodeposition and membrane systems or even ion exchange process [4]. Among these technologies, adsorption may be considered as preferable in many cases due to its outstanding simplicity, high efficiency, low investment, and potential recovery and reuse of metals [5]. In recent years, investigations have been carried out for low cost, non-

* Corresponding author.
E-mail address: liyf@lzu.edu.cn (Y. Li).

1385-8947/$ - see front matter © 2012 Elsevier B.V. All rights reserved.
http://dx.doi.org/10.1016/j.cej.2012.06.082

conventional adsorbents which provide high removal efficiency as well as specific interactions with the targeted toxic metals [6].

Chelating and chelating magnetic resins represent an important category of promising adsorbents due to their highly selective, efficient and easily regenerable relative to other types of adsorbent materials [7,8]. Several chelating resins containing a variety of attached chemical functional groups have been reported for developing low cost, non-conventional adsorbents which provide high removal efficiency as well as specific interactions with the targeted toxic metals [9–13]. Generally, the amino/carboxyl group on an adsorbent has been found one of the most effective chelate functional groups for adsorption or removal of heavy metal ions from an aqueous solution. It is also widely accepted that nitrogen-containing functional groups act as adsorption sites for heavy metals [14–16]. The mechanism of adsorption includes mainly ionic interactions (chemical interactions) and electrostatic interactions (physical interactions) between metal cations and chelating magnetic resins. Ethylenediaminetetraacetic acid (EDTA) is a hexadentate ligand that provides both carboxylate and amine functions. For the EDTA modified materials, the amino and two hydroxyl groups on each EDTA in the repeating unit can act as reactive sites to capture metals [17–19]. On the other hand, magnetic modified chelating resins are superior due to their relatively fast, easy separation and collection by magnetic control and higher uptake capacity compared to chelating polymers [8,20,21].

In our previous work, we prepared EDTA chelating polystyrene resin (PS-EDTA) which showed good absorptive effects for metal ions. The purpose of the present study was devoted to develop and characterize an magnetic modified PS-EDTA for Cr(VI) ions removal from water. Fourier transform infrared spectroscopy (FT-IR), scanning electron microscopy (SEM), BET specific surface area (BET), vibrating sample magnetometry (VSM) and X-ray diffraction (XRD) were used investigate the properties of the sorbent, such as microstructure, surface morphology, magnetism and surface area of the sorbent. A series of batch experiments by raw and magnetic PS-EDTA resins was carried out and the effects of the process parameters such as contact time, pH, initial Cr(VI) concentration and dosage of the resins on Cr(VI) removal were investigated. In order to better understand the adsorption characteristic, some isotherm and kinetic models were employed to evaluate the sorption process. X-ray photoelectron spectroscopy (XPS) was explored to probe the interaction of the chromium and sorbent. Further, a conceptual model for the adsorption of Cr(VI) by the magnetic resin is proposed to illustrate the mechanism.

2. Experimental

2.1. Preparation of adsorbent

The chloromethylated polystyrene grafted by EDTA (PS-EDTA) was magnetic modified by coprecipitation method. The PS-EDTA was synthesized and provided by our laboratory [22]. About 2 g of PS-EDTA was soaked in 50 mL of $FeCl_3{\cdot}6H_2O$ (0.02 mol) solution in a beaker and rotated for 2 h, and then was transferred to a 250 mL three-necked glass flask. $FeCl_2{\cdot}4H_2O$ (0.01 mol) dissolved in 50 mL of deionized water was added in as followed under a nitrogen atmosphere with vigorous stirring at room temperature. The aqueous NaOH solution (25 mL, 10 M) was then slowly added to the solution, which immediately turned black. The reaction mixture was stirred for 1 h at room temperature and then heated in a water bath at 90 °C with continuous stirring for 2 h.

Black magnetic beads were separated from the mixture by filtration and rinsed thoroughly with distilled water and acetone to neutral. Samples were dried in a vacuum desicator for few days for the obtainment of magnetic modified PS-EDTA resin.

2.2. Preparation of Cr(VI) solutions

Stock solution (1000 mg/L) of Cr(VI) was prepared by dissolving 2.829 g of potassium bichromate ($K_2Cr_2O_7$) in 1000 mL of water. This solution was further diluted to prepare different working concentrations. The pH of the solution was adjusted with 0.1 M HCl and 0.1 M NaOH solutions. The concentration of Cr(VI) was determined spectrophotometrically at 540 nm by the colored complex developed between the anions and diphenylcarbazide in acid solution [20,23].

2.3. Batch adsorption experiments

Batch experiments were conducted in 250 mL conical flasks by shaking at 120 rpm in a water bath shaker. A specific amount of dry resins (raw resin or magnetic resin) is added in 100 mL of aqueous Cr(VI) solution, and then stirred for a predetermined period (found out from the kinetic studies) at 30 °C in a temperature controlled shaker incubator. Afterwards, the resins (raw resin or magnetic resin) were separated, and the supernatant was collected for Cr(VI) measurement. Adsorption isotherm study is carried out with different initial Cr(VI) concentration (5–1000 mg/L). The adsorption capacity of the resin and the percentage removal of Cr(VI) are calculated using the following Eqs. (1) and (2) respectively

$$Q_t = \frac{(C_o - C_e)\cdot V/1000}{W} \tag{1}$$

$$\%\ \text{removal of mental} = \frac{C_i - C_o}{C_i} \times 100 \tag{2}$$

where Q_e (mg/g) is the adsorption capacity; C_i (mg/L) and C_e (mg/L) are the initial and equilibrated metal ion concentrations, respectively, V (L) is the volume of added solution and W (g) is the mass of the adsorbent (dry).

The kinetic experiments were carried out as the effect of contact time with time ranges of 5–600 min. The process of metal ion removal from an aqueous phase by any adsorbent can be explained by using kinetic models and examining the rate-controlling mechanism of the adsorption process such as chemical reaction, diffusion control and mass transfer.

2.4. Desorption experiments

For desorption studies, 0.10 g of resin was loaded with metal ions using 100 mL (30 mg/L) metal ion solution at 30 °C, pH 4.0 and contact time of 10 h. The agitation rate was fixed as 120 rpm. After adsorption, resins were collected, and gently washed with distilled water to remove any unabsorbed metal ions. Then, the resins were agitated with 20 mL of NaOH solution (0.1–1 M). The final concentration of Cr(VI) in the aqueous phase was determined. The percentage of Cr(VI) desorption from resins was calculated from the amount of metal ions adsorbed on resins and the final concentration of metal ions in the desorption medium, which was calculated as

$$\%\ \text{percentage desorption} = \frac{m_{NaOH}}{m_{ad}} \times 100\% \tag{3}$$

where m_{NaOH} is the metal ion desorbed to the NaOH solution (mg) and m_{ad} is the metal ion adsorbed onto the resin (mg). To test the reusability of the resin, this adsorption–desorption cycle was repeated ten times by using the same affinity adsorbent. The regeneration efficiency was calculated using

$$\%\ \text{regeneration efficiencye} = \frac{m_i}{m_1} \times 100 \tag{4}$$

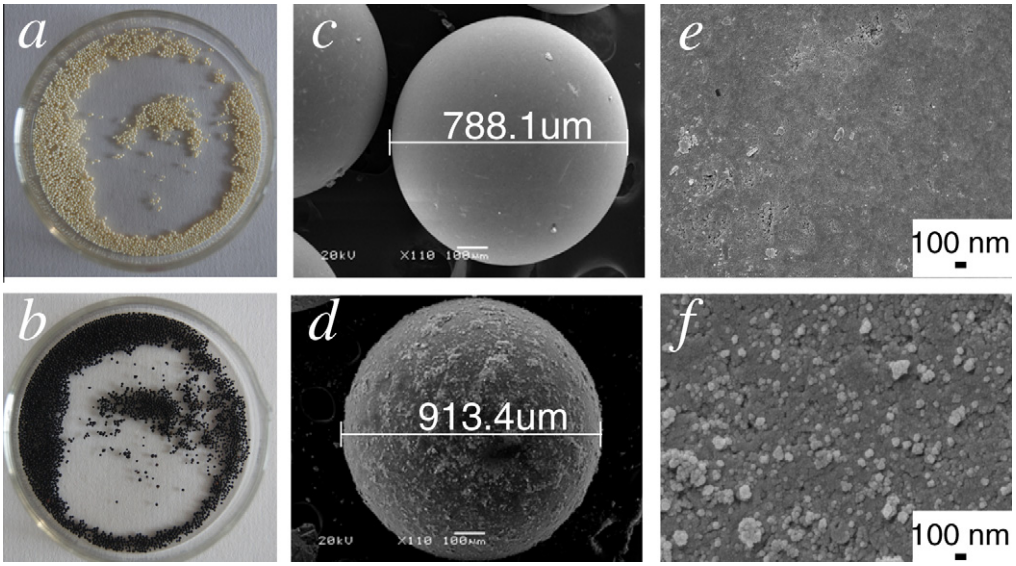

Fig. 1. The macro- and micro-structure of the resins: digital pictures of the (a) raw PS-EDTA resins and (b) magnetic modified ones; SEM images of the (c and e) raw resin and (d and f) magnetic resin.

where m_i is the uptake of Cr(VI) in the second to tenth cycle, respectively, and m_1 is the uptake of Cr(VI) in the first cycle.

2.5. Characterization

The adsorbents were characterized by FT-IR, SEM, BET, VSM and XRD. The FT-IR spectra of PS-EDTA and magnetic PS-EDTA were recorded with a Nicolet Magna-IR 550 spectrophotometer between 4000 and 400 cm^{-1} using the KBr pellet technique. For SEM observation, the size and morphology of the beads were characterized using a JEOC JSM-6701F scanning electron microscope at accelerating voltages of 5 kV. The BET of PS-EDTA and magnetic PS-EDTA were measured by the N_2 adsorption–desorption technique using a Micromeritics Chemisorb 2750 surface area analyzer. Magnetic properties were detected by a vibrating sample magnetometer (Lakeshore 7304). For XRD, the structural parameters of beads were investigated by using an SHLMADZU-6000X equipment.

XPS was used to figure out the mechanism of the removal of Cr(VI). The XPS spectra of magnetic PS-EDTA before and after Cr(VI) adsorption at pH 4 were recorded by an X-ray photoelectron spectrometer (VG Scientific Escalab 210-UK) equipped with an Mg Kα X-ray source (1253.6 eV protons). The X-ray source was run at a reduced power of 300 W. All the binding energies were referenced to the C1s peak at 285.0 eV to compensate for the surface charging effects.

The concentration of Cr(VI) was determined using a UV–vis spectrophotometer (UV-754 N shanghai, China) at 540 nm. The pH of solutions was determined using a HANNA pH meter. A thermostat oscillators (HaiSheng Da HQD 150L) was used for shaking all of the solutions.

3. Results and discussion

3.1. Absorbent characterization

The finality products all show as opaque, uniform and black beads (Fig. 1b). From the SEM (Fig. 1c–f), the number average diameter of the magnetic PS-EDTA (913.4 μm, Fig. 1d) was bigger than that of PS-EDTA (788.1 μm, Fig. 1c). The surface morphologies of the resins are much different. The surface of PS-EDTA is relatively smooth (Fig. 1c) and it is yellowish[1] (Fig. 1a) while the color of magnetic PS-EDTA is black (Fig. 1b) and there are many embossments on the surface of magnetic modified PS-EDTA (Fig. 1d). This property is favorable for producing good adsorption. Further, for the magnetic resin (Fig. 1f), many particles at the size of 20–30 nm in the surface were observed, which may exist as Fe_3O_4 nanoparticles. It is also considered helpful for mass transfer of Cr(VI) ions, which will be explained by XPS in Section 3.6.

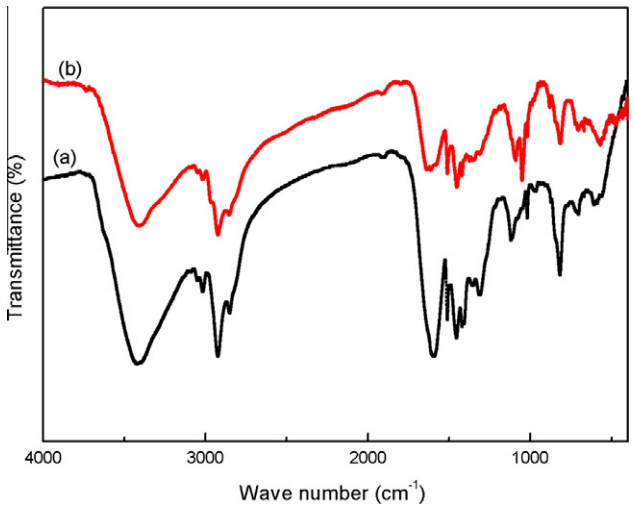

Fig. 2. The FT-IR spectra of (a) raw PS-EDTA resin and (b) magnetic PS-EDTA resin.

The surface area calculated from the method of BJH Adsorption cumulative volume of pores shows that magnetic PS-EDTA (77.98 m^2/g) exhibits a higher surface area than PS-EDTA resin (48.55 m^2/g). Meanwhile, the magnetic PS-EDTA (0.27 cm^3/g) shows a decreased pore volume compared to raw PS-EDTA (0.32 cm^3/g). It was possibly as a result of improved roughness on the surface of magnetic resin after magnetic modification.

The FTIR spectra are shown in Fig. 2. The broad bands at 3451 (Fig. 1a) and 3450 (Fig. 1b) are due to the characteristic stretching vibration of N—H bond in amino (—NH_2) and imino (—NH—groups,

[1] For interpretation of color in Figs. 2, 5 and 7–10, the reader is referred to the web version of this article.

strongly indicating the presence of a large amount of amino and imino groups in the raw and magnetic modified PS-EDTA resin [1]. The two peaks at 2928 (Fig. 1a) and 2930 cm^{-1} (Fig. 1b) can confirm the existence of abundant methylene in the polymer main chain. The two sharp peaks around 820 cm^{-1} and 1100 cm^{-1} might be assigned to the stretching vibration of =CH bond and the various amine, respectively. These band positions do not change after modification, suggesting that the basic structure of PS-EDTA remains constant. The vibration bands at 590 cm^{-1} are newly observed, which can be attributed to Fe—O stretching vibrations. The peak around 1611 cm^{-1} in spectrum Fig. 1a is attributed to υ_{as} of aminocarboxylicacid groups. A blue shift of this spectral peak position at 1643 cm^{-1} in spectrum Fig. 1b was observed along with the magnetic modification of PS-EDTA, which might be related to the complexing of ferric ion and aminocarboxylicacid. Thus, the analysis of the diagnostic regions confirms the successful magnetic modification of PS-EDTA.

XRD pattern of magnetic modified PS-EDTA resin is shown in Fig. 3. Form XRD, six characteristic peaks for Fe_3O_4 (2θ = 30.1°, 35.5°, 43.3°, 53.4°, 57.2°and 62.5°), marked by their indices ((220), (311), (400), (422), (511), and (440)), were observed. It indicated the existence of iron oxide particles (Fe_3O_4) and the resin has magnetic properties, which can be used for the magnetic separation.

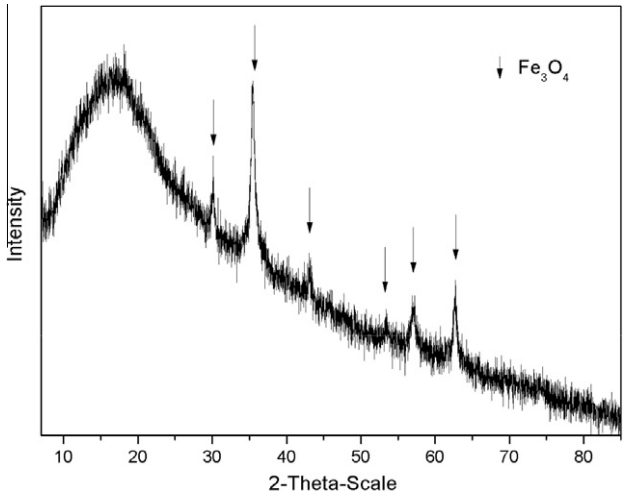

Fig. 3. XRD pattern of magnetic PS-EDTA resin.

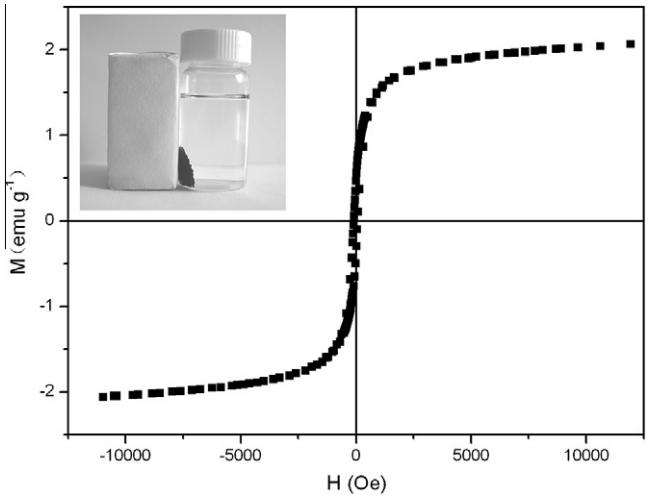

Fig. 4. VSM magnetization curve of magnetic PS-EDTA resin and its magnetic separation from aqueous solution (inset).

The VSM (Fig. 4) shows the magnetic PS-EDTA had a saturated magnetization of 2.07 emu/g, and this magnetic susceptibility value is sufficient for this resin to be used in wastewater treatment.

3.2. Cr(VI) adsorption

The adsorption trends of Cr(VI) on the EDTA chelating resins (raw and magnetic resin) in aqueous solution were investigated as a function of PH, contact time, initial metal ion concentration and resin dosage.

3.2.1. Effect of pH

The extractability of the anions from the solution phase is pH dependent because of its effect on the solubility of the metal ions, concentration of the counter ions on the functional groups of the adsorbent and the degree of ionization of the adsorbate during reaction [23]. The effect of pH on Cr(VI) removal by PS-EDTA and magnetic PS-EDTA was investigated in the pH ranges of 2–12 at 30 °C for 6 h. As shown in Fig. 5, the highest uptake capacities of the resins were achieved at pH 3–4. At pH < 2, the decrease in adsorption capacity may be attributed to the competitive adsorption between Cl^- anions. At higher pH of 4–12, the adsorption of Cr(VI) onto the both resins decreased sharply. It can be explained by the following reasons: (1) For the both resins, the functional —NH_2 and —NH— groups in the raw and magnetic PS-EDTA resin which are considered as active sites for the adsorption of Cr(VI) can undergo protonation to —NH_3^+ and —NH_2^+, then Cr(VI) anions existing as $HCrO_4^-$ and CrO_4^{2-} adsorption occurred. In case of chromate ions, they are known to exist in the following equilibrium states [24–26]:

$$H_2CrO_4 \leftrightarrow HCrO_4^- + H^+, \quad k_1 = 1.21 \tag{5}$$

$$Cr_2O_7^{2-} + H_2O \leftrightarrow 2HCrO_4^-, \quad k_2 = 35.5 \tag{6}$$

$$HCrO_4^- \leftrightarrow CrO_4^{2-} + H^+, \quad k_3 = 3 \times 10^{-7} \tag{7}$$

$$HCr_2O_7^- \leftrightarrow Cr_2O_7^{2-} + H^+, \quad k_4 = 0.85 \tag{8}$$

The extent of protonation will be dependent on the solution pH. The behavior that both PS-EDTA and magnetic PS-EDTA resins display a decrease in the uptake value as pH increases can be explained on the basis of the lower extent of protonation of amino group with

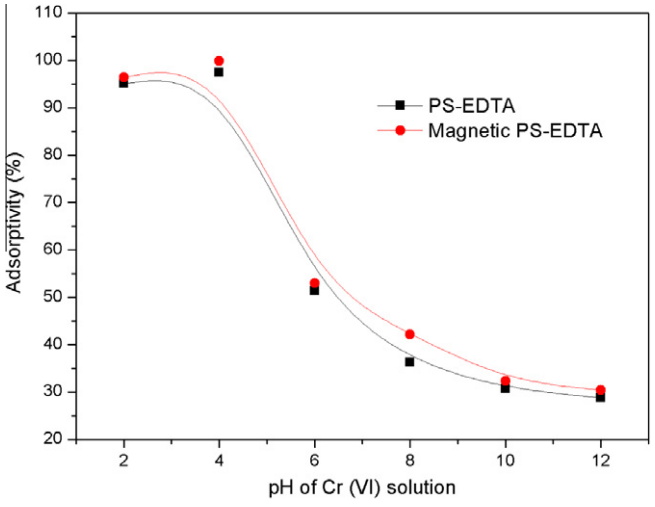

Fig. 5. The effect of pH on the adsorption of Cr(VI) ions into raw and magnetic modified PS-EDTA (initial concentration of Cr(VI) ions: 30 mg/L; resins feed: 1 g/L; adsorption time: 5 h; *T*: 30 °C).

rising pH. (2) For the magnetic resins, low acidic conditions also caused the surface of the Fe_3O_4 nanoparticles to be protonated to a higher extent, which resulted in a strong attraction between the negatively charged Cr(VI) complex ions and the positively charged surface[27]. Further, the two-valent iron (Fe^{2+}) on the surface of magnetic resin is a moderate reducing reagent, which can react with chromic acid for Cr(VI) reduction and these reactions are favored at low pH [28]. The reduction is attributed to the following:

$$Fe^{2+} + H_2CrO_4 + H^+ \rightarrow Fe^{3+} + H_3CrO_4 \quad (9)$$

$$Fe^{2+} + H_3CrO_4 + H^+ \rightarrow Fe^{3+} + H_4CrO_4 \quad (10)$$

$$Fe^{2+} + H_4CrO_4 + H^+ \rightarrow Fe^{3+} + Cr(OH)_3 + H_2O \quad (11)$$

Thus, the effect of pH on the removal of Cr(VI) by magnetic resin was influenced not only by the protonation of $—NH_2$ groups but also by the protonation of Fe_3O_4 nanoparticles and reducing action of Fe^{2+}, which resulting a higher adsorption of Cr(VI) compared to raw PS-EDTA resin.

3.2.2. Effect of contact time

The effect of contact time on the adsorption of the Cr(VI) was investigated in the time ranges of 5 min–10 h under pH 4 at 30 °C. The change in the uptake of Cr(VI) by the given resin (raw or magnetic resins) as a function of time are shown in Fig. 6. The uptake-time curves show that the maximum uptake follows the order magnetic resin > raw resin at all time intervals. The uptake rates of both resins were fast within 80 min. For PS-EDTA, value of 99.3% of the maximum uptake was achieved around 8 h while almost total Cr(VI) was removed by magnetic resin and equilibrium is achieved at around 5 h. To be sure of the best adsorption conditions at higher concentration levels and to obtain equilibrium at the solid/liquid interface, all the experiments were carried out with 10 h of contact time. The shorter time period required to attain equilibrium and higher uptake of magnetic resin suggest an excellent affinity of the magnetic resin for Cr(VI) from aqueous solution and the behavior could be explained by improved surface roughness, more active sites and the existence of reducing action of Fe^{2+}.

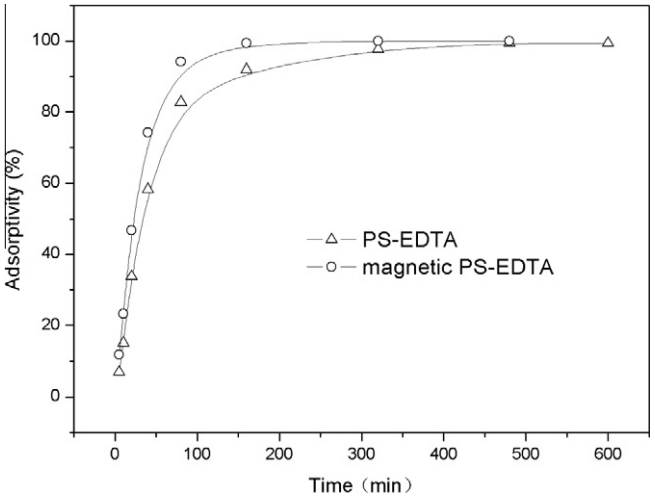

Fig. 6. The effect of contact time on the uptake of Cr(VI) ions by raw and magnetic modified PS-EDTA resins (initial concentration of Cr(VI) ions: 30 mg/L; resins feed: 1 g/L; pH 4.0; *T*: 30 °C).

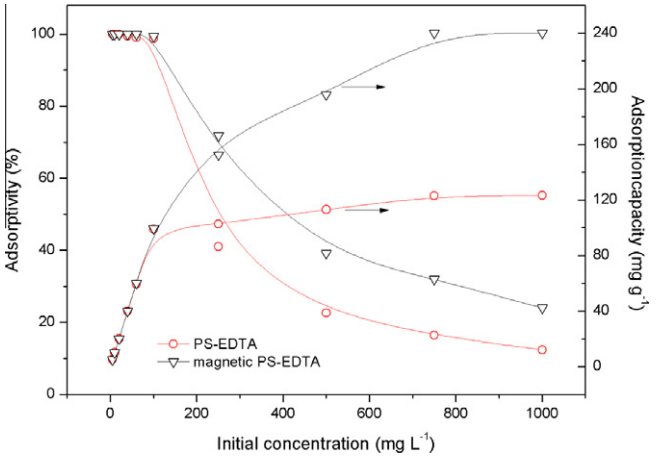

Fig. 7. The effect of the initial Cr(VI) concentration on the uptake of Cr(VI) ions by raw and magnetic modified PS-EDTA resins (resins feed: 1 g/L; pH 4.0; adsorption time: 10 h; *T*: 30 °C).

3.2.3. Effect of initial Cr(VI) concentration

Initial Cr(VI) concentration was adjusted in the ranges of 5–1000 mg/L for adsorption on the EDTA chelating resins (raw and magnetic PS-EDTA) under pH 4 at 30 °C for 10 h as shown in Fig. 7. The increasing initial Cr(VI) concentration resulted in an increase in the Cr(VI) on the both resins due to abundant active groups and increased driving force towards the active sites on the beads [29]. The adsorption capacity of Cr(VI) by the both resins increased rapidly with increase in the Cr(VI) concentration in the range of 5–100 mg/L, while increased slowly as the ion concentration was higher than 100 mg/L. almost total Cr(VI) was removed at the low initial concentration of 5–20 mg/L for raw resin and 5–40 mg/L for magnetic resin. The adsorption capacity on the both resins in 1000 mg/L of Cr(VI) solution reached the maximum values of 123.2 mg/g and 240.2 mg/g while the effective values (12.3% and 24.0%, respectively) is much lower. Both of the sorption capacity and removal percentage of magnetic modified resin are higher than raw PS-EDTA due to more active sites on the resin's surface after modification. These results indicate that the magnetic modified PS-EDTA was more effective for Cr(VI) removal and this magnetic chelating resin was fit for being used to treat micro-polluted water with Cr(VI) of low concentrations(<40 mg/L).

3.2.4. Effect of resin dosage

The resin dosage of 0.02, 0.06, 0.10, 0.14, 0.18 and 0.20 g were used in 30 mg/L Cr(VI) solutions under pH 4 to test their effects on Cr(VI) removal by PS-EDTA and magnetic modified PS-EDTA. As shown in Fig. 8, the percentage removal of Cr(VI) by both resins increased with increasing amount of adsorbents. This behavior can be attributed to the increased availability of adsorption sites. Almost complete removal of Cr(VI) was observed at adsorbent dosages of 1 g/L for magnetic resin. By comparison, more adsorbent dosage of 1.80 g/L was required to complete adsorption of Cr(VI) for raw PS-EDTA resin. It might be due to increased adsorption sites, higher surface area and introduced reducing agent after magnetic modification, all of which means more powerful removal for Cr(VI). As consequence, an adsorbent dosage of 1.0 g/L was selected as the optimum value for 30 mg/L Cr(VI) removal by magnetic PS-EDTA and used for the remaining adsorption studies.

3.3. Adsorption isotherms

Equilibrium data, commonly known as adsorption isotherms, are important in the basic design of adsorption systems, and are

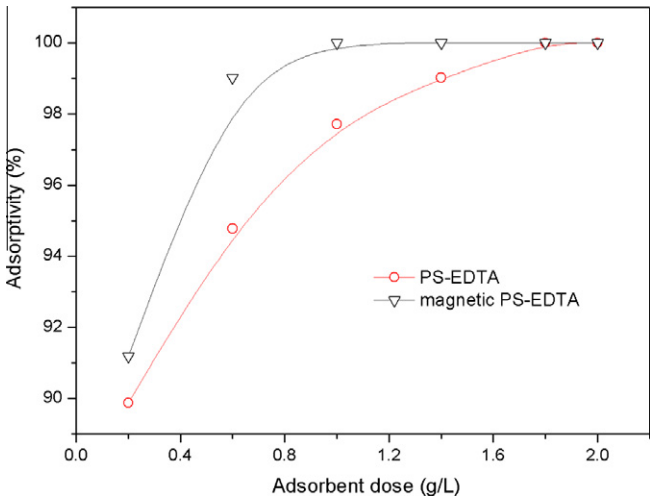

Fig. 8. The effect of dosage on the uptake of Cr(VI) ions by raw and magnetic modified PS-EDTA resins (initial concentration of Cr(VI) ions: 30 mg/L; pH 4.0; adsorption time: 10 h; *T*: 30 °C).

critical in optimizing the use of adsorbents. To optimize the design of an adsorption system for removing Cr(VI) from solutions, it is essential to establish the most appropriate correlation for the equilibrium curves [30]. Several adsorption isotherms originally used for gas phase adsorption are available and readily adopted to correlate adsorption equilibria in heavy metals adsorption. Some well-known ones are Freundlich, Langmuir, Temkin, Redlich–Paterson and Sips equations [31]. In this study, The equilibrium data for the adsorption of Cr(VI) on both resins was tested with Langmuir, Freundlich and Tempkin adsorption isotherm models. The isotherm constants for the three models were obtained by linear regression method. The modeled quantitative relationship between Cr(VI) concentration and the sorption process, the calculated correlation coefficients and standard deviations are listed in Table 1, and also three resins' sorption isotherm are compared through the calculated constants and regression data for various adsorption isotherms, which are listed in Table 2.

The Langmuir model assumes that a monomolecular layer is formed when adsorption takes place without any interaction between the adsorbed molecules [32], and takes the following linear form:

$$\frac{C_e}{Q_e} = \frac{1}{bQ_m} + \frac{C_e}{Q_m} \tag{12}$$

where C_e is the equilibrium concentration (mg/L), Q_e the amount of metal ion sorbed (mg/g), Q_m is Q_e for a complete monolayer (mg/g), b is a constant related to the affinity of the binding sites (L/mg).

The experimental data (Table 1) exhibited high correlation (R^2 is 0.9980 and 0.9918 for the raw and magnetic resin systems, respectively) with Langmuir model for both raw and magnetic PS-EDTA resins. Further, the values (Table 2) of Q_m (123.05 and 250.00 mg/g for raw and magnetic resins, respectively) were close to the experimental data (123.15 and 240.23 mg/g) of adsorption capacity. Through the above analysis, it can be considered that Langmuir isotherm equation can be used to describe adsorption of Cr(VI) by both raw and magnetic resin, which illustrates a monolayer adsorption process. The Q_m of magnetic resin was remarkably higher than the Q_m value of raw resin, indicating a good adsorption on magnetic resin.

The Freundlich isotherm theory says that the ratio of the amount of solute adsorbed onto a given mass of sorbent to the concentration of the solute in the solution is not constant at different concentrations. The heat of adsorption decreases in magnitude with increasing the extent of adsorption [33]. The linear Freundlich isotherm is commonly expressed as follows:

$$\log Q_e = \log K_f + \frac{1}{n}\log C_e \tag{13}$$

where K_f ($mg^{1-1/n}\,L^{1/n}\,g^{-1}$) and n (g/L) are the Freundlich constants characteristics of the system, indicating the relative adsorption capacity of the adsorbent related to the bonding energy and the adsorption intensity, respectively.

To determine the maximum sorption capacity, it is necessary to operate with constant initial concentration C_o and variable weights of sorbent, thus log Q_m is the extrapolated value of log Q for $C = C_o$ [34]. According to Halsey [35]:

$$K_f = \frac{Q_m}{C_o^{1/n}} \tag{14}$$

From the corresponding parameters of Freundlich isotherm summarized in Table 1, high correlation coefficients ($R^2 > 0.95$) and low standard diversion (Standard deviation < 0.03) can be observed for both resins. However, the maximum sorption capacity computed using Halsey expression (Table 2) are far lower than the experimental adsorbed amounts at equilibrium corresponding to the plateau of the sorption isotherms. This means that the equilibrium isotherms cannot be described by the Freundlich model.

Tempkin isotherm equation assumes that the heat of adsorption of all the molecules in the layer decreases linearly with the coverage of molecules due to the adsorbate–adsorbate repulsions and the adsorption of adsorbate is uniformly distributed and that the fall in the heat of adsorption is linear rather than logarithmic [36]. The linearized Tempkin equation is given by the following equation:

$$Q_e = B_T \ln A_T + B_T \ln C_e \tag{15}$$

where $B_T = (R_T)/b_T$, T is the absolute temperature in K and R is the universal gas constant (8.314 J/(mol K)). The constant b_T is related to the heat of adsorption, A_T is the equilibrium binding constant (L/min) corresponding to the maximum binding energy. The slope and the intercept from a plot of Q_e versus ln C_e determine the isotherm constants A_T and b_T.

The constants of Tempkin isotherm can be obtained from the slope and intercept of a straight line plot of Q_e versus ln C_e. Tempkin constants are given in Table 1. The Cr(VI) sorption onto the raw

Table 1
Isothermal model equations for Cr(VI) sorption on the resins.

Mathematical model	The resin	Equation	Correlation coefficient	Standard deviation
Langmuir	Raw resin	$C_e/Q_e = 0.0081C_e + 0.0454$	0.9980	0.0440
	Magnetic resin	$C_e/Q_e = 0.004C_e + 0.038$	0.9918	0.0389
Freundlich	Raw resin	$\log Q_e = 0.123 \log C_e - 1.741$	0.9582	0.0249
	Magnetic resin	$\log Q_e = 0.123 \log C_e - 2.015$	0. 9595	0.0283
Тёмкин	Raw resin	$Q_e = 9.396\ln C_e + 59.022$	0.9857	2.536
	Magnetic resin	$Q_e = 19.164\ln C_e + 102.178$	0.8842	17.763

Table 2
Isotherm constants and regression data for various adsorption isotherms for adsorption of Cr(VI) onto the resins.

The resin	Langmuir		Freundlich		Tёмкин			
	Q_m (mg/g)	b (L/mg)	k_f ((L/mg)$^{1/n}$)	n (mg/L)	Q_m (mg/g)	A_T (L/min)	B_T (J/mol)	b_T
Raw resin	123.457	0.178	0.0182	8.145	0.0426	534.802	9.396	268.253
Magnetic resin	250	0.105	0.00966	8.161	0.0226	206.809	19.164	131.518

PS-EFTA resin is more appropriately described by the Tempkin isotherm model because of a much higher correlation coefficient (R^2 is 0.9857 and 0.8842 for the raw and magnetic resin systems, respectively) and a much lower standard diversion. It means that sorption of Cr(VI) on raw PS-EDTA resin was mainly via chemical adsorption, and after magnetic modification, the chemical adsorption was not the dominating adsorb style.

3.4. Kinetics of Cr(VI) adsorption

The rate of metal sorption is an important factor and prerequisite for determining the reactor design and process optimization for a successful practical application. The rate kinetics of Cr(VI) adsorption on raw and magnetic PS-EDTA resins at initial metal ion concentration of 30 mg/L were analyzed using pseudo-first order, pseudo-second order and Elovich kinetic models. The modeled quantitative relationship between time and the sorption process, calculated correlation coefficients and standard deviations are listed in Table 3.

Lagergren showed that the rate of adsorption of solute on the adsorbent is based on the adsorption capacity and followed a pseudo first-order equation which is often used for estimating k_{ad} considered as mass transfer coefficient in the design calculations [37]. The integrated rate law after application of the initial condition of $Q_t = 0$ at $t = 0$, becomes a linear equation as given by the following equation:

$$\log(Q_e - Q_t) = \log Q_e - \frac{k_{ad}t}{2.303} \tag{16}$$

where Q_e and Q_t are the amounts of Cr(VI) adsorbed (mg/g) at equilibrium time and at any instant of time, t, respectively, and k_{ad} (L/min) is the rate constant of the pseudo first order sorption.

The pseudo second-order kinetic model Eq. (17) [38] is given as:

$$\frac{t}{Q_t} = \frac{t}{Q_e} + \frac{1}{h} \tag{17}$$

where $h = k_2 Q_e^2$ that can be regarded as the initial sorption rate as t approaches 0. The k_2 (g/(mg min)) is the second-order rate constant.

Elovich equation is a rate equation based on the adsorption capacity describing adsorption on highly heterogeneous adsorbents [39]. Eq. (18) is simplified by assuming $\alpha\beta \gg t$ and by applying the boundary conditions $Q_t = 0$ at $t = 0$ and $Q_t = Q_t$ at $t = t$:

$$Q_t = \frac{1}{\beta}\ln(\alpha\beta) + \frac{1}{\beta}\ln t \tag{18}$$

where α (mg/(g min)) is the initial adsorption rate and β (g/mg) is the desorption constant related to the extent of the surface coverage and activation energy for chemisorption.

The calculated kinetic parameters for pseudo first-order, second-order and Elovich kinetic models are listed in Table 4. The experimental Q_e values are in agreement with the calculated values using both pseudo first-order and pseudo second-order kinetics. Based on the obtained coefficients of determination (R^2) from Table 3, the pseudo second-order equation was the model that leads to the best fit for the experimental kinetic data.

The results indicate that the physical adsorption and reducing action are increased after magnetic modification and mechanisms of such as; ion exchange, chelation and physical adsorption are all involved in the adsorption process for magnetic resin. Further, from Table 4, the larger rate constants of the pseudo first-order (k_{ad}), second-order value (k_2) and Elovich (α) suggest that adsorption systems with magnetic resin will required a shorter time to achieve a specific fractional uptake [40].

The sorption process for both resins also fit Elovich kinetic models with correlation coefficient more than 0.96 and standard diversion not very high. It means that sorption of Cr(VI) on both resins involves chemical adsorption, and the sorbent surface is not only one type functional groups, which is the same with the result described above.

3.5. Rate controlling step analysis

The prediction of the rate controlling step is an important factor to be considered in the adsorption process [41]. The contact time variation experiment can be used to study the rate controlling step in the adsorption process [42]. For a solid–liquid sorption process, the solute transfer is usually characterized by external mass transfer (boundary layer diffusion), or intraparticle diffusion, or both. As they happen simultaneously, the slower one of the two stages would be the rate controlling step. The most commonly used technique for identifying the mechanism involved in the adsorption process is by fitting an intraparticle diffusion plot. According to Weber and Morris [43], the intraparticle diffusion model is expressed as

$$Q_t = K_{id}t^{0.5} + C_i \tag{19}$$

where Q_t (mg/g) is the amount of metal ion adsorbed at time t (min) and K_{id} is intraparticle diffusion rate (mg/(g min$^{1/2}$)). C_i is the intercept of stage i, which gives an idea of the thickness of the boundary layer, i.e., the larger the intercept, the greater the boundary layer

Table 3
Kinetic model equations for Cr(VI) sorption onto the resins.

Mathematical model	The resins	Equation	Correlation coefficient	Standard deviation
Pseudo first-order	Raw resin	$\log(Q_e - Q_t) = -0.00555t + 1.357$	0.9531	0.0699
	Magnetic resin	$\log(Q_e - Q_t) = -0.0139t + 1.467$	0.9939	0.0367
Pseudo second-order	Raw resin	$t/Q_t = 0.0311t + 1.179$	0.9956	0.226
	Magnetic resin	$t/Q_t = 0.0304t + 0.721$	0.9926	0.178
Elovich	Raw resin	$Q_t = 8.061\ln t - 12.519$	0.9731	2.119
	Magnetic resin	$Q_t = 8.380\ln t - 10.531$	0.9663	2.474

Table 4
Calculated kinetic parameters for pseudo first order, second order and Elovich kinetic models.

The resin	Q_e, exp (mg/g)	Pseudo first-order		Pseudo second-order		Elovich		
		$k_{ad} \times 10^{-3}$ (L/min)	Q_e, Cal (mg/g)	$k_2 \times 10^{-4}$ (g/mg min)	h (mg/g min)	Q_e, Cal (mg/g)	α (mg/g min)	β (g/mg)
Raw resin	29.80	12.78	22.73	8.21	0.848	32.15	1.71	0.124
Magnetic resin	30.00	32.08	29.32	12.85	1.39	32.89	2.39	0.119

effect. If intraparticle diffusion is involved in the adsorption process, then the plot of Q_t versus $t^{0.5}$ will be linear; and if these lines pass through the origin, then the rate controlling process is due only to the intraparticle diffusion [44].

In this model, it is assumed that the mechanism for a solid–liquid adsorption process involves the following three steps: (i) bulk diffusion, which involves the movement of metal ions from aqueous phase through the hydrodynamic boundary layer film of the solid; (ii) intraparticle diffusion, where the metal ions move through the interior solid surface transport of the adsorbate within the pores of the adsorbent (particle diffusion); (iii) adsorption at the active sites. The third step is considered to be very rapid and therefore it cannot said to be the rate controlling step. Thus, the overall rate of adsorption is controlled by either film or intraparticle diffusion, or a mixture of both [30]. The plot of Q_t vs $t^{0.5}$ as shown in Fig. 9 represents the different stages of adsorption. The initial curved portion of the plot indicates a boundary layer effect, while the second linear portion is due to intraparticle or pore diffusion. The third portion indicates the final equilibrium stage where intraparticle diffusion starts to slow down because of the extremely low adsorbate concentrations in the solution. For both resins, the plots do not go through origin. It means that the adsorption involved intraparticle diffusion, but it was not the only rate controlling step. A slope K_{id}, intercept C_i and correlation coefficient R^2 were determined from the second linear portion of the plot, as listed in Fig. 9. The intercept and correlation coefficient values observed indicated that the contribution of the surface sorption in the rate controlling step was greater for magnetic resin.

The McKay plot establishes whether the rate controlling step of mass transfer is film diffusion or particle diffusion [45]. The plot is based on the assumption that adsorption follows Fick's law which reduces to the follow form at longer times of adsorption

$$\log\left(1-\frac{Q_t}{Q_e}\right) = \log\frac{6}{\pi^2} + \left(\frac{-D_2\pi^2}{a^2}\right)t \quad (20)$$

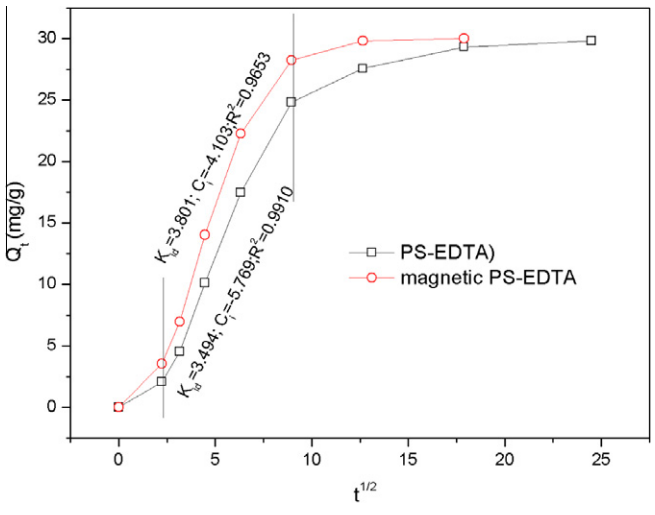

Fig. 9. The intraparticle diffusion plots of Cr(VI) onto raw and magnetic PS-EDTA resins.

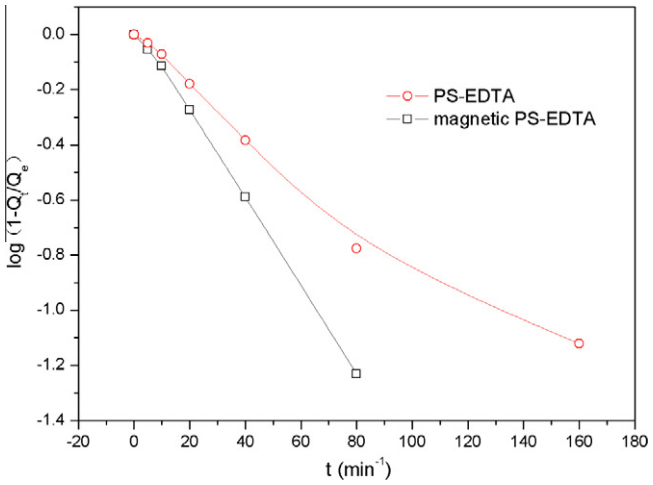

Fig. 10. The McKay plots of Cr(VI) onto raw and magnetic PS-EDTA resins.

where D_2 (cm^2 s^{-1}) is the particle diffusion coefficient.

McKay plots of $\log(1 - Q_t/Q_e)$ vs t for both resins are shown in Fig. 10. It can be observed that the plot for unmodified PS-EDTA was much scattered, indicating an intraparticle diffusion adsorption. However, linearity was found for magnetic modified resin, which indicates that film diffusion becomes the rate controlling step. This is the same with the result described above and it should be due to the improved surface roughness resulted by the introduction of Fe_3O_4 nanoparticles after modification. The Fe_3O_4 nanoparticles loaded on the resin improved more active sites, meanwhile, these Fe_3O_4 nanoparticles obstructed the pores of the resin, which lead to the surface adsorption of Cr(VI).

3.6. Sorption mechanism

XPS has often been used to identify the interaction of an adsorbate with the surface functional groups on an adsorbent because the creation of a chemical bond between them changes the distribution of the electrons around the corresponding atoms [46,47]. The XPS wide scan spectra of the sorbents before and after adsorption are shown in Fig. 11a, while the high-resolution spectra of Cr 2p, Fe 2p, and N 1s are shown in Fig. 11b–d.

From Fig. 11a, the major peaks at binding energy of 712, 531 and 399 eV are clearly observed for both magnetic resins (virgin and Cr-loaded sorbents), which are assigned for Fe 2p, O 1s and N 1s, respectively. A small peak at 577 eV is observed after chromate adsorption (Cr-loaded sorbent). It indicates a small amount of chromate in the sorbent after adsorption.

Fig. 11b displays the high-resolution scan of Cr 2p. From the deconvolution of the curve, it can be observed that the major peak at the binding energy of 577 eV consisted of two peaks assigned to Cr(III) and Cr(VI) at 577.8 and 580.4 eV, respectively. Cr(VI) constitutes the basic structure unit of the adsorbate (K_2CrO_4). The Cr(VI) peak indicates the loading of the adsorbate on the resin, whereas the Cr(III) peak reflects the possible reduction of Cr(VI) to Cr(III) on the resin surface.

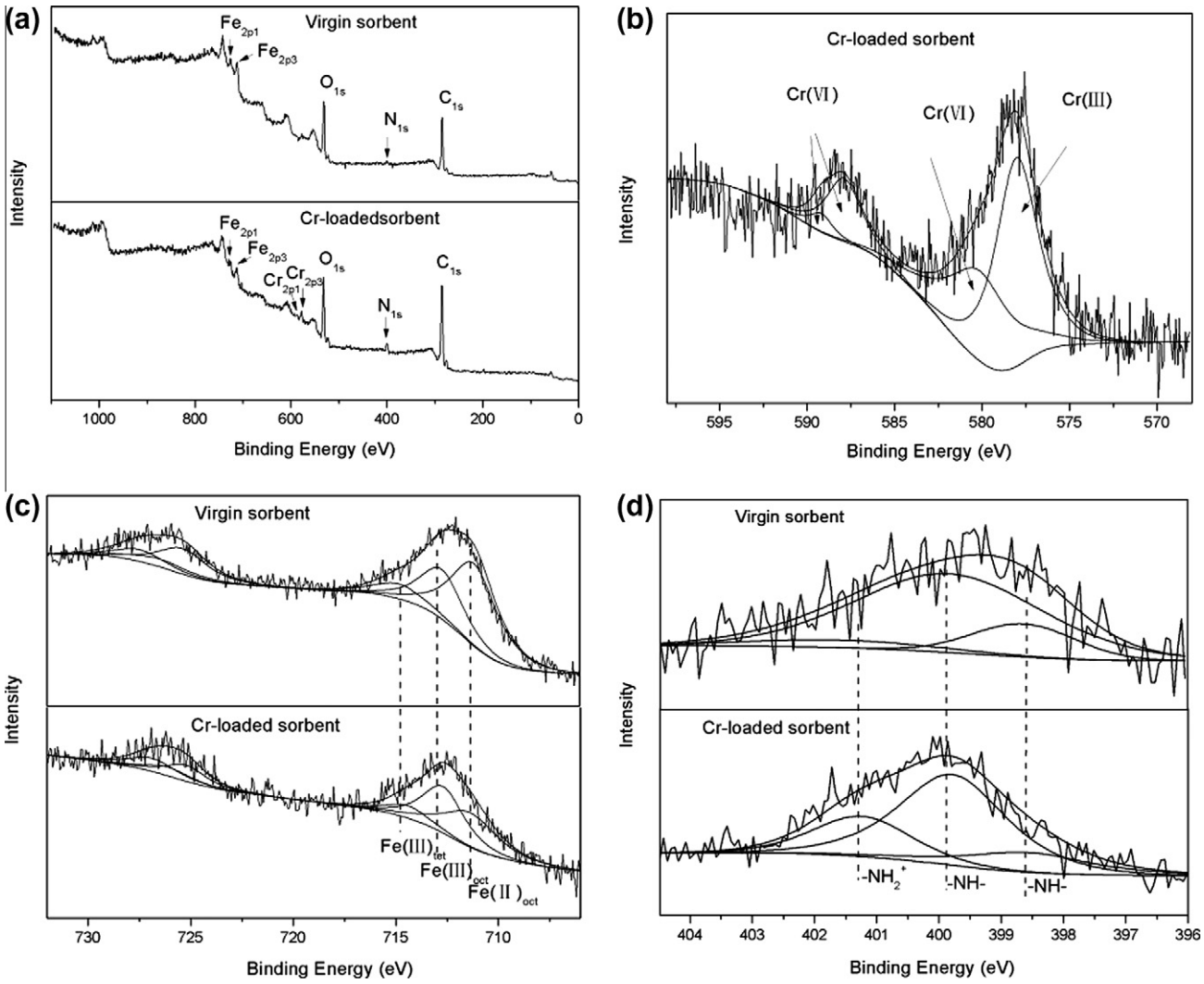

Fig. 11. XPS wide scan of the virgin and Cr-loaded magnetic resin, Cr 2p core-level spectrum of the Cr-loaded magnetic resin, Fe 2p and N 1s core-level spectra of the virgin and Cr-loaded magnetic resin.

Fig. 11c shows the high-revolution scan of Fe 2p for both virgin and Cr-loaded sorbents. It can be observed from virgin sorbent that the deconvolution of the Fe 2p spectrum produces three different peaks: octahedral ferrous ($Fe(II)_{oct.}$), octahedral ferric ($Fe(III)_{oct.}$) and tetrahedral ferric ($Fe(III)_{tet.}$) peaks at 711.3, 712.8 and 714.8 eV, respectively. With the adsorption of Cr(VI) on the magnetic resin, the same three peaks can still be observed but the ratio of Fe(II)/Fe(III) decreased from 1.33 to 0.65. The results indicate that the process of solid redox reaction might occur during the adsorption process which involves the oxygen functionalities with the reduction of Cr(VI) and oxidation of Fe(II).

The N 1s core-level XPS spectra of the resin before and after Cr(VI) sorption were presents in Fig. 11d. For the spectrum of the resin before sorption, the peaks at binding energy of 398.5 and 399.7 eV are attributed to the nitrogen in the —NH— and the peak at 401.3 eV is assigned to $—NH_2^+$ [48]. About 7% amine groups were protonated before adsorption. After anion Cr(VI) was adsorbed on the resin at pH 4, the area ratio of the peak at 401.3 eV increased to 24%, which might be attributed to the protonated nitrogen atom on the resin and adsorption of negative Cr(VI). The protonated amine groups are responsible for Cr(VI) sorption. The amine groups were first protonated at pH 4, and then adsorbed the negative Cr(VI) ions via electrostatic attraction.

On the basis of above experimental and instrumental analyses, the mechanism of chromate removal by the magnetic PS-EDTA resin is proposed as shown in Fig. 12. The metal oxides and amine groups are first protonated, followed by bonding of anionic Cr(VI). Some of the adsorbed Cr(VI) species are further reduced to Cr(III), and divalent iron in the Fe_3O_4 provides electrons in the chemical reduction of Cr(VI).

3.7. Resins regeneration

For potential practical application of the resins, it is important to examine the possibility of desorption and reusing the resins. 20 mL NaOH with various concentration of 0.01–1 M was used as the desorbing agent for the recovery of Cr(VI) from metal-loaded magnetic resin. Desorption experiments were performed maintaining the process condition similar to the batch experiments. As shown in Fig. 13, the desorption ratio of metal ions increased as NaOH concentration increased. This can be interpreted according to the deprotonation of the chromate species. However, the desorption ratio of the Cr(VI) was almost the same in the range over the concentration of 0.5 M. Hence, the best concentration of NaOH was determined to be 0.5 M for economical process. Complete desorption was not possible, perhaps due to the

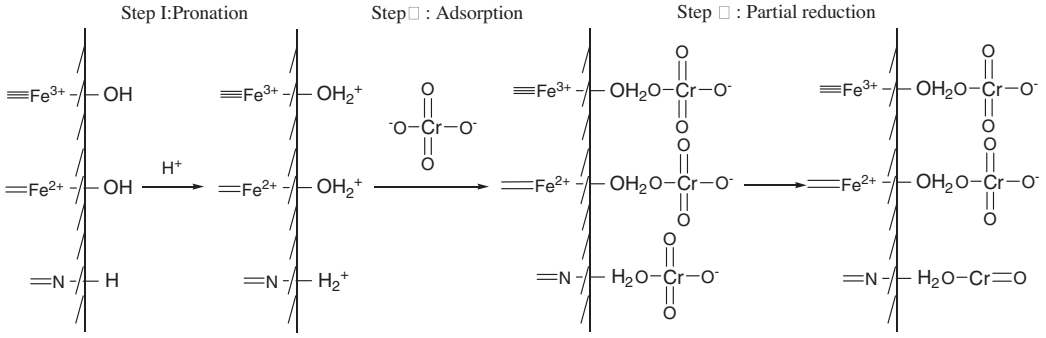

Fig. 12. A proposed mechanism for the adsorption of Cr(VI) onto magnetic PS-EDTA resin.

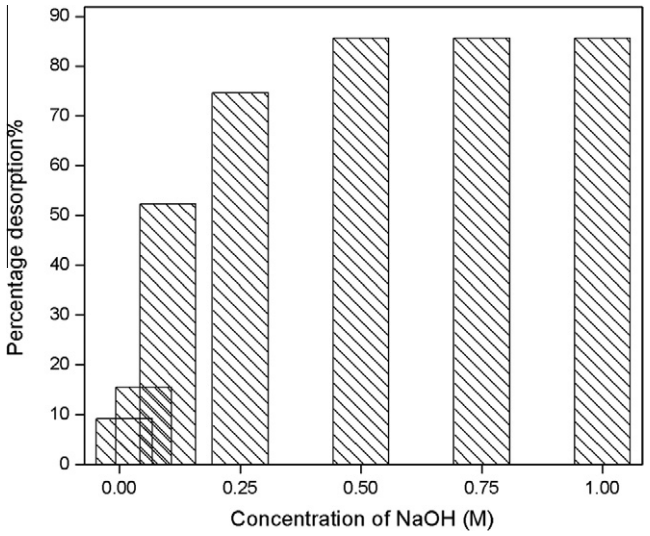

Fig. 13. Desorption of Cr(VI) from metal loaded magnetic PS-EDTA resin by 0.01–1 M NaOH (20 mL).

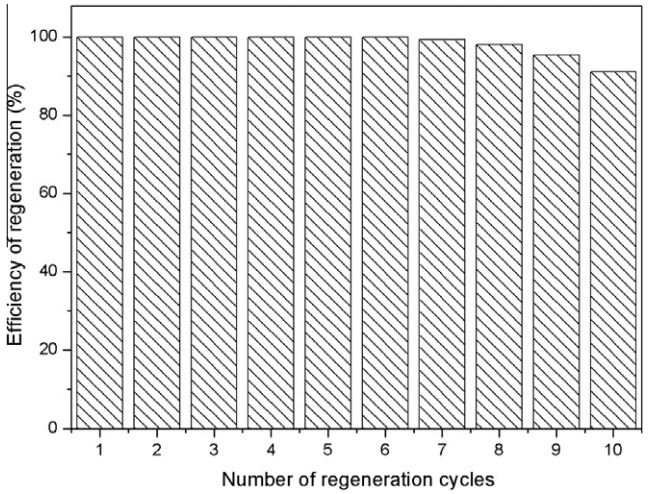

Fig. 14. Repeated adsorption of Cr(VI) using magnetic PS-EDTA resin (initial concentration of Cr(VI) ions: 30 mg/L; resins feed: 0.1 g; pH 4.0; contact time: 10 h; *T*: 30 °C).

involvement of reduction of the Cr(VI) ions and non-electrostatic forces between the resin and the Cr(VI) ions [49]. The regenerated resin was reused for up to ten adsorption–desorption cycles and the results are illustrated in Fig. 14. It was found that the efficiency of regeneration was more than 91% after the tenth cycle. These results showed that the magnetic modified PS-EDTA can be successfully regenerated and repeatedly used in Cr(VI) ions adsorption studies without appreciable losses in their adsorption capacities.

4. Conclusions

Magnetic chelating resin with EDTA functionality (magnetic PS-EDTA) was prepared and characterized by means of FT-IR, SEM, BET, VSM and XRD. The adsorption properties of the raw and magnetic modified PS-EDTA resin toward Cr(VI) ions were evaluated via batch method. Various factors affecting the uptake behavior such as pH, contact time, initial concentration of the metal ions and dosage of resins on Cr(VI) removal were investigated. The results showed that the magnetic modified resin has higher adsorption capacity (240.23 mg/g) and shorter adsorption equilibrium time (5 h) for Cr(VI) compared with the raw resin (123.15 mg/g, 10 h). The equilibrium data were analyzed using the Langmuir, Freundlich, and Tempkin isotherm models among which Langmuir isotherm model was found to be suitable for the Cr(VI) adsorption. The kinetic parameters were evaluated utilizing the pseudo first-order, pseudo second-order and Elovich kinetic models. The adsorption kinetics followed the mechanism of the pseudo second-order equation for magnetic resins, evidencing that both chemical and physical adsorption are involved in adsorption process. The mechanism was further identified by fitting intraparticle diffusion and McKay plots. The result indicates film diffusion was the rate-limiting step and intraparticle diffusion was also involved in adsorption. The interaction of Cr(VI) with the surface functional groups on magnetic resin was characterized via XPS, which proved that reduction of Cr(VI) by Fe_3O_4 nanoparticle on the resin occurred, while the electrostatic interaction between protonated amine groups and Cr(VI) anion played an important role in the adsorption. The mechanism of Cr(VI) adsorption is also illustrated by a proposed conceptual model. Regeneration of magnetic PS-EDTA obtained was achieved by using 0.5 M NaOH and subsequent use of the regenerated PVA-EDTA resin end up in practically no change in sorption effectiveness.

Acknowledgements

The authors gratefully acknowledge financial supports from the National Major Specific Program of Science and Technology on Controlling and Administering of Water's pollution (2009ZX07212-001-04), Key Research Program of Gansu Province (2GS064-A52-036-02, GS022-A52-082), as well as the helps from associate professor Lincheng Zhou.

Appendix A. Supplementary material

Supplementary data associated with this article can be found, in the online version, at http://dx.doi.org/10.1016/j.cej.2012.06.082.

References

[1] J.L. Gardea-Torresdey, K.J. Tiemann, V. Armendariz, L. Bess-Oberto, R.R. Chianelli, J. Rios, J.G. Parsons, G. Gamez, Characterisation of Cr(VI) binding and reduction to Cr(III) by the agricultural byproducts of Avena monida (oat) biomass, J. Hazard. Mater. B80 (2000) 175–188.

[2] S. Basha, Z.V.P. Murthy, B. Jha, Biosorption of hexavalent chromium by chemically modified seaweed, Cystoseira indica, Chem. Eng. J. 137 (2008) 480–488.

[3] H. Yao, L. Guo, B.H. Jiang, J. Luo, X. Shi, Oxidative stress and chromium(VI) carcinogenesis, J. Environ. Pathol. Toxicol. Oncol. 27 (2008) 77–88.

[4] P. Miretzkya, A. Fernandez Cirellib, Cr(VI) and Cr(III) removal from aqueous solution by raw and modified lignocellulosic materials: a review, J. Hazard. Mater. 180 (2010) 1–19.

[5] B.E. Reed, W. Lin, M.R. Matsumoto, J.N. Jensen, Physicochemical processes, Water Environ. Res. 69 (1997) 444–461.

[6] D. Park, S.R. Lim, Y.S. Yun, J.M. Park, Selective adsorption of chromiumVI in industrial wastewater using low-cost abundantly available adsorbents, Bioresour. Technol. 99 (2008) 8810–8818.

[7] K.Z. Elwakeel, A.A. Atia, A.M. Donia, Removal of Mo(VI) as oxoanions from aqueous solutions using chemically modified magnetic chitosan resins, Hydrometallurgy 97 (2009) 21–28.

[8] M. Moniera, D.M. Ayad, Y. Wei, A.A. Sarhanb, Sarhanb, Adsorption of Cu(II), Co(II), and Ni(II) ions by modied magnetic chitosan chelating resin, J. Hazard. Mater. 177 (2010) 962–970.

[9] B.L. Rivas, S.A. Pooley, M. Luna, K.E. Geckeler, Synthesis of water-soluble polymers containing sulfonic acid and amine moieties for the recovery of metal ions using ultrafiltration, J. Appl. Polym. Sci. 82 (2001) 22–30.

[10] S. Cavus, G. Gurdag, Noncompetitive removal of heavy metal ions from aqueous solutions by poly[2-(acrylamido)-2-methyl-1-propanesulfonic acid co-itaconic acid] hydrogel, Ind. Eng. Chem. Res. 48 (2009) 2652–2658.

[11] R.X. Liu, H.X. Tang, B.W. Zhang, Removal of Cu(II), Zn(II), Cd(II) and Hg(II) from wastewater by poly (acrylaminophosphonic) type chelating fiber, Chemosphere 38 (1999) 3169–3179.

[12] T.A. Kurniawan, G.Y.S. Chan, W.H. Lo, S. Babel, Physico-chemical treatment techniques for wastewater laden with heavy metals, Chem. Eng. J. 118 (2006) 83–98.

[13] B.J. Gao, Y.C. Gao, Y.B. Li, Preparation and chelation adsorption property of composite chelating material poly(amidoxime)/SiO_2 towards heavy metal ions, Chem. Eng. J. 158 (2010) 542–549.

[14] P.A. Kumar, S. Chakraborty, M. Ray, Removal and recovery of chromium from wastewater using short chain polyaniline synthesized on jute fiber, Chem. Eng. J. 141 (2008) 130–140.

[15] R. Ansari, N.K. Fahim, Application of polypyrrole coated on wood sawdust for removal of Cr(VI) ion from aqueous solutions, React. Funct. Polym. 67 (2007) 367–374.

[16] S.K. Das, A.R. Das, A.K. Guha, A study on the adsorption mechanism of mercury on Aspergillus versicolor biomass, Environ. Sci. Technol. 41 (2007) 8281–8287.

[17] F.V. Pereira, L.V.A. Gurgel, L.F. Gil, Removal of Zn^{2+} from aqueous single metal solutions and electroplating wastewater with wood sawdust and sugarcane bagasse modified with EDTA dianhydride (EDTAD), J. Hazard. Mater. 176 (2010) 856–863.

[18] E. Repo, J.K. Warchol, T.A. Kurniawan, M.E.T. Sillanpaa, Adsorption of Co(II) and Ni(II) by EDTA- and/or DTPA-modified chitosan: kinetic and equilibrium modeling, Chem. Eng. J. 161 (2010) 73–82.

[19] O.K. Júnior, L.V.A. Gurgel, R.P. Freitas, L.F. Gil, Adsorption of Cu(II), Cd(II), and Pb(II) from aqueous single metal solutions by mercerized cellulose and mercerized sugarcane bagasse chemically modified with EDTA dianhydride (EDTAD), Carbohydr. Polym. 77 (2009) 643–650.

[20] X. Hua, J. Wang, Y. Liu, X. Li, G. Zeng, Z. Bao, X. Zeng, A. Chen, F. Long, Adsorption of chromium (VI) by ethylenediamine-modified cross-linked magnetic chitosan resin: isotherms, kinetics and thermodynamics, J. Hazard. Mater. 185 (2011) 306–314.

[21] E.B. Denkbas, E. Kiliçay, C. Birlikseven, E. Öztürk, Magnetic chitosan microspheres: preparation and characterization, React. Funct. Polym. 50 (2002) 225–232.

[22] L.Q. Yang, Y.F. Li, L.Y. Wang, Y. Zhang, X.J. Ma, Z.F. Ye, Preparation and adsorption performance of a novel bipolar PS-EDTA resin in aqueous phase, J. Hazard. Mater. 180 (2010) 98–105.

[23] A.I. Zouboulis, K.A. Kydros, K.A. Matis, Removal of hexavalent chromium anions from solutions by pyrite fines, Water Res. 29 (1995) 1755–1760.

[24] A.K. Sengupta, D. Clifford, Important process variables in chromate ion exchange, Environ. Sci. Technol. 20 (1986) 149–155.

[25] A.K. Sengupta, D. Clifford, S. Subramonian, Chromate ion-exchange process at alkaline pH, Water Res. 20 (9) (1986) 1177–1184.

[26] G. Bayramoglu, G. Celik, M. Yilmaz, M.Y. Arica, Modification of surface properties of Lentinus sajor-caju mycelia by physical and chemical methods: evaluation of their Cr^{6+} removal efficiencies from aqueous medium, J. Hazard. Mater. 119 (2005) 219–229.

[27] S.K. Prabhakaran, K. Vijayaraghavan, R. Balasubramanian, Removal of Cr(VI) ions by spent tea and coffee dusts: reduction to Cr(III) and biosorption, Ind. Eng. Chem. Res. 48 (2009) 2113–2117.

[28] W.X. Zhang, Nanoscale iron particles for environmental remediation: an overview, J. Nanopart. Res. 5 (2003) 323–332.

[29] A.Y. Dursun, A comparative study on determination of the equilibrium, kinetic and thermodynamic parameters of biosorption of copper(II) and lead(II) ions onto pretreated Aspergillus niger, Biochem. Eng. J. 28 (2006) 187–195.

[30] S. Chen, Q. Yue, B. Gao, X. Xu, Equilibrium and kinetic adsorption study of the adsorptive removal of Cr(VI) using modified wheat residue, J. Colloid Interface Sci. 349 (2010) 256–264.

[31] J. Febrianto, A.N. Kosasih, J. Sunarso, Y.H. Ju, N. Indraswati, S. Ismadji, Equilibrium and kinetic studies in adsorption of heavy metals using biosorbent: a summary of recent studies, J. Hazard. Mater. 162 (2009) 616–645.

[32] I. Langmuir, The adsorption of gases on plane surfaces of glass, mica and platinum, J. Am. Chem. Soc. 40 (1918) 1361–1403.

[33] H.M.F. Freundlich, Over the adsorption in solution, Z. Phys. Chem. 57 (1906) 385–471.

[34] R. Djeribi, O. Hamdaoui, Sorption of copper (II) from aqueous solutions by cedar sawdust and crushed brick, Desalination 225 (2008) 95–112.

[35] G.D. Halsey, The role of surface heterogeneity in adsorption, Adv. Catal. 4 (1952) 259–269.

[36] P.A. Kumara, M. Ray, S. Chakrabortya, Adsorption behaviour of trivalent chromium on amine-based polymer aniline formaldehyde condensate, Chem. Eng. J. 149 (2009) 340–347.

[37] R.B. Garcia-Reyes, R.R.M. Jose, Adsorption kinetics of chromium(III) ions onagro-waste materials, Bioresour. Technol. 101 (2010) 8099–8108.

[38] Y.S. Ho, G. McKay, The kinetics of sorption of basic dyes from aqueous solution by sphagnum moss peat, Can. J. Chem. Eng. 76 (1998) 822–827.

[39] S.H. Chien, W.R. Clayton, Application of Elovich equation to the kinetics of phosphate release and sorption on soils, Soil. Sci. Soc. Am. J. 44 (1980) 265–268.

[40] B.H. Hameed, M.I. El-Khaiary, Malachite green adsorption by rattan sawdust: isotherm kinetic and mechanism modelling, J. Hazard. Mater. 159 (2008) 574–579.

[41] M. Sarkar, P.K. Acharya, B. Battacharya, Modeling the adsorption kinetics of some priority organic pollutants in water from diffusion and activation energy parameters, J. Colloid Interface Sci. 266 (2003) 28–32.

[42] B.S. Inbaraj, N. Suluchana, Basic dye adsorption on a low cost carbonaceous sorbent, kinetics and equilibrium studies, Ind. J. Chem. Tan. 9 (2002) 201–208.

[43] W.J. Weber, J.C. Morris, Kinetics of adsorption on carbon from solution, J. San. Eng. Div. ASCE 89 (1963) 31–39.

[44] J.H. Huang, X.M. Wang, X. Deng, Synthesis, characterization, and adsorption properties of phenolic hydroxyl group modified hyper-cross-linked polymeric adsorbent, J. Colloid Interface Sci. 337 (2009) 19–23.

[45] M.H. Kalavathy, T. Karthikeyan, S. Rajgopal, L.R. Miranda, Kinetic and isotherm studies of Cu(II) adsorption onto H_3PO_4-activated rubber wood sawdust, J. Colloid Interface Sci. 292 (2005) 354–362.

[46] S.B. Deng, Y.P. Ting, Polyethylenimine-modified fungal biomass as a high-capacity biosorbent for Cr(VI) anions: sorption capacity and uptake mechanisms, Environ. Sci. Technol. 39 (2005) 8490–8496.

[47] L. Niu, S. Deng, G. Yu, J. Huang, Efficient removal of Cu(II), Pb(II), Cr(VI) and As(V) from aqueous solution using an aminated resin prepared by surface-initiated atom transfer radical polymerization, Chem. Eng. J. 165 (2010) 751–757.

[48] Y.M. Zheng, S.F. Lim, J.P. Chen, Preparation and characterization of zirconium-based magnetic sorbent for arsenate removal, J. Colloid Interface Sci. 338 (2009) 22–29.

[49] V. Singh, S. Tiwari, A.K. Sharma, R. Sanghi, Removal of lead from aqueous solutions using Cassia grandis seed gum-graft-poly(methylmethacrylate), J. Colloid Interface Sci. 316 (2007) 224–232.